Photonic crystal slot waveguide Spectrometer for detection of Methane

Swapnajit Chakravarty*[a], Wei-Cheng Lai[b], Xiaolong Wang[a], Cheyun Lin[b], Ray T. Chen[b],
[a]Omega Optics Inc., 10306 Sausalito Drive, Austin, TX, USA 78759; [b]Dept. of Electrical and Computer Engineering, University of Texas, 10100 Burnet Road Bldg. 160, Austin, TX USA 78758

ABSTRACT

Defect engineered photonic crystals, with sub-micron dimensions have demonstrated high sensitivity to trace volumes of analytes; however exact identification of analyte through spectroscopic signatures had not been demonstrated. We demonstrate a 300micron long photonic crystal slot waveguide device which combines slow light phenomenon in photonic crystal waveguides with large optical field intensity in a low index narrow slot at the center of the photonic crystal waveguide for highly sensitive spectroscopic detection of methane on-chip at 100 parts per million (ppm) or 0.2% permissible exposure limit. Photonic crystal slot waveguide provides a factor of 1000 reduction in interaction length compared to free-space infrared spectroscopy leading to enhanced optical absorption by analytes in the optical path. By measuring absorption differences in presence and absence of methane, near-infrared absorption spectrum of methane is determined.

Keywords: photonic crystal slot waveguide, on-chip absorption spectroscopy, near-infrared integrated spectrometer, methane sensor.

*swapnajit.chakravarty@omegaoptics.com; phone 1 512 996-8833; fax 1 512-873-7744; omegaoptics.com

1. INTRODUCTION

Pollution of air in the United States and the world can have serious and wide-ranging effects on environment and human health. Contamination of the environment and the fatal danger to human health by hazardous materials and greenhouse gases is an omnipresent problem and is a concern of several departments of the U.S. Government. The threat posed by global terrorism should also be underlined. Due to enormous significance of keeping the environment clean and free from intentional and unintentional contamination, an elaborate in-situ and highly sensitive sensing technology with remote monitoring capacity is an absolute necessity.

Infrared (IR) spectroscopy is widely used as a simple and reliable technique for quality control and analysis. Infrared spectroscopy does not require costly analyte labeling, which makes the technique very attractive for sensing and identification compared to other spectroscopy methods. Most commercially available optical absorption spectrometers are large, heavy, power consuming and expensive. Furthermore, they can detect only a few species at a time. Systems that detect multiple gases are prohibitively expensive and not portable. A primary requirement is a sample cell into which the analyte gas is routed for measurement, thereby substituting for in-situ monitoring. Optical fiber based remote monitoring systems need to be very long to achieve detection sensitivities mandated by US Occupational Safety and Health Administration (OSHA).

2. PRINCIPLE OF OPERATION

The photonic crystal slot waveguide is shown schematically in Figure 1 (a). It consists of a triangular lattice of photonic crystal air holes and a slot waveguide etched into silicon on a silicon-on-insulator (SOI) wafer. The measurement principle is based on Beer-Lambert-Bouguer absorption method. According to this technique, the transmitted intensity I is given by

$$I = I_0 \exp(-\gamma \alpha L) \qquad (1)$$

where I_0 is the incident intensity, α is the absorption coefficient of the medium, L is the interaction length and γ is the medium-specific absorption factor determined by dispersion enhanced light-matter interaction. In conventional systems,

Integrated Optics: Devices, Materials, and Technologies XV, edited by Jean Emmanuel Broquin, Gualtiero Nunzi Conti, Proc. of SPIE Vol. 7941, 79410K · © 2011 SPIE
CCC code: 0277-786X/11/$18 · doi: 10.1117/12.873299

L must be large to achieve a suitable sensitivity of the measured I/I_0. For lab-on-chip systems, L must be small, hence γ must be large. Mortensen et al showed [1] using perturbation theory that

$$\gamma = f \times \frac{c/n}{v_g} \quad \text{..... (2)}$$

where c is the velocity of light in free space, v_g is the group velocity in the medium of effective index n and f is the filling factor denoting the relative fraction of the optical field residing in the analyte medium. Equation 2 shows that slow light propagation (small v_g) significantly enhances absorption. Furthermore, greater the electric field overlap with the analyte, greater the effective absorption by the medium.

Photonic Crystal (PC) devices have demonstrated high sensitivity to small changes in refractive index of ambient [2]. Photonic crystals can also slow light significantly from its velocity in free space. Fig. 1(b) shows the dispersion relation of a typical guided mode in a photonic crystal waveguide. The slow light region in the photonic band gap with low group velocity $v_g = d\omega/d\beta$ is circled in red. It has been demonstrated that the group velocity of propagating light can be reduced by a **factor of 100** in the slow light region [3]. Slot waveguides have attracted considerable attention over the past few years due to their ability to confine light with high intensity in narrow low-index slots between high index ridges [Fig. 1(c)] [4]. This has the effect of increasing f as well as lowering n in Equation 2. Calculations show that electric field intensity $|E|^2$ is increased by a **factor of 10** in the slot compared to planar waveguide evanescent coupling [5]. The combined effects of slow group velocity and high optical field intensity in the slot lead to **a factor of 1000 reduction in interaction length** required to sense analytes in photonic crystal slot waveguides. The miniaturization by significant reduction in interaction length compared to commercial spectrometers will enable in-situ measurements and analysis. Our demonstrated device is ~300μm long. By measuring the difference of photonic crystal slot waveguide transmission spectra in presence and absence of analyte, the near-IR absorption spectrum of analyte is determined.

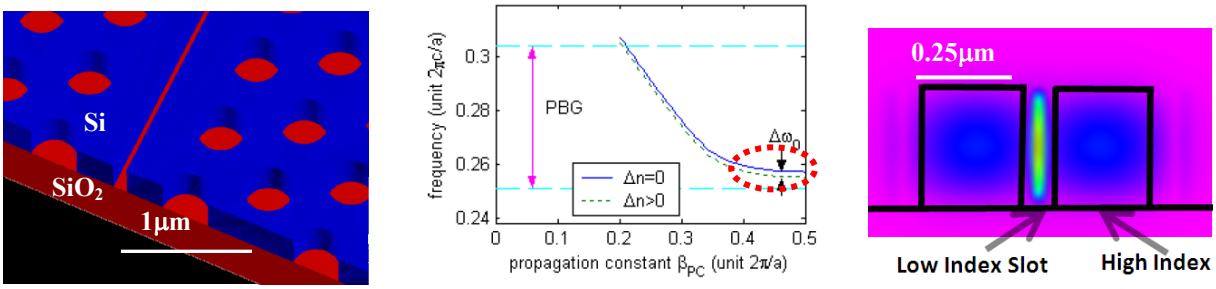

(a) (b) (c)

Figure 1: (a) Schematic of a photonic crystal slot waveguide [**Legend: Silicon (blue), Silicon Dioxide (red)**] (b) Dispersion curve of guided mode in a photonic crystal slot waveguide. The low group velocity region is circled in red. (c) Simulated electric field intensity $|E|^2$ profile in a slot waveguide showing high intensity in the low-index slot.

3. DEVICE DESIGN FOR CHIP-INTEGRATED METHANE SPECTROSCOPY

Horizontally, the mode in Fig. 1(b) in the photonic crystal waveguide (PCW) is guided by photonic bandgap, while vertically, it is still index confined. It is important to ensure that the photonic crystal defect slot mode is completely confined in the photonic bandgap in addition to providing high electric field confinement in the slot.

In Fig. 2, the dispersion diagram of the final structure is shown. The blue shaded area denotes the region above the light line for top cladding air, while the green shaded region denotes the area above the light line for bottom cladding silicon dioxide. As observed from the band diagram, multiple modes are observed in the band gap below the light line of silicon dioxide. However, modes other than the selected one (shown by the dotted black line) are either significantly propagating in the dielectric or are not confined in the photonic band gap. The ideal mode, as shown, is confined in the photonic band gap and has a significant fraction of the energy propagating in the slot. This is important to ensure sufficient optical overlap exists between the analyte filling the slot, in this case methane gas, and the guided optical mode with low propagation loss.

A W1.3 photonic crystal slot waveguide was fabricated. The photonic crystal waveguide is fabricated by removing a complete row of air-holes from the input to the output. A W1 photonic crystal waveguide is one where a single row of air holes has been removed from the input to the output. Thus W1= $\sqrt{3}a$, where a is the lattice constant of the triangular lattice. Wx denotes a PC waveguide where the width of the waveguide is modified by a fraction x. In our final design,

therefore, the width of the photonic crystal waveguide is $1.3\times\sqrt{3}a$. Other design parameters are: air hole radius = $0.25a$, slot width=$0.2a$, waveguide length=300μm. From Fig. 2, slow light guided mode propagates at normalized frequency a/λ=0.275. The peak of methane absorbance spectrum occurs at 1.665μm, hence from the above normalized frequency for slow light propagation, a=457.8nm. We design at the normalized frequency for which group index n_g=40. At this wavelength, a=461nm.

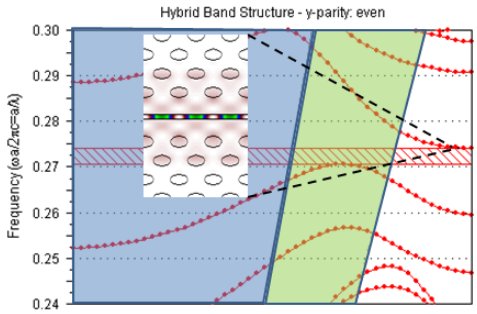

Figure 2: (a) Photonic Crystal Slot Waveguide simulation, showing the defect mode in the inset at the intersection of the dotted black lines. The blue shaded area denotes the area above the light line in air (top cladding) while the green shaded area denotes the area above the light line in silicon dioxide (bottom cladding).

4. DEVICE FABRICATION

The fabrication process follows these procedures: First, a 50nm oxide layer is formed by thermal oxidation on top of an SOI wafer; second, 140nm thick e-beam photoresist is spin coated and patterned by e-beam lithography, including the input/output waveguides and the photonic crystal holes. Then, the oxide layer is etched by RIE, which serves as the hard mask for the waveguide layer etching; in the last step, the silicon layer is etched downed to the buried oxide. The entire process is shown in figure 3.

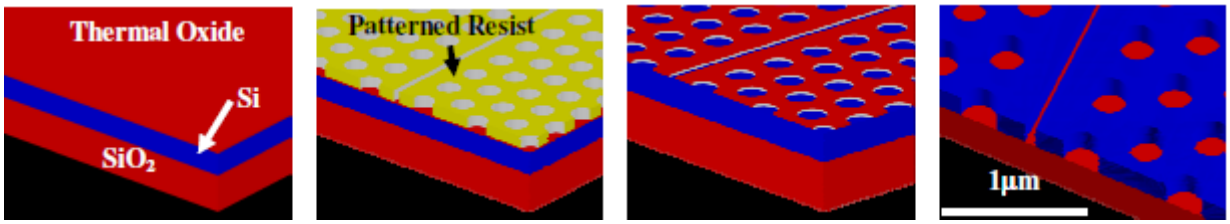

Figure 3: Fabrication steps of a PC slot waveguide (a) Growth of thermal oxide (b) E-beam Resist (ZEP-520A) patterning (c) Transfer of resist pattern to thermal oxide by RIE using CHF_3 followed by resist strip (d) Transfer of pattern from thermal oxide to Si by RIE in HBr and Cl_2. [**Legend: Silicon (blue), Silicon Dioxide, SiO_2 (red)**]

Fabrication was done using a combination of e-beam lithography and dry reactive ion etching. Scanning electron micrograph (SEM) images are shown in Fig. 4 for fabricated devices.

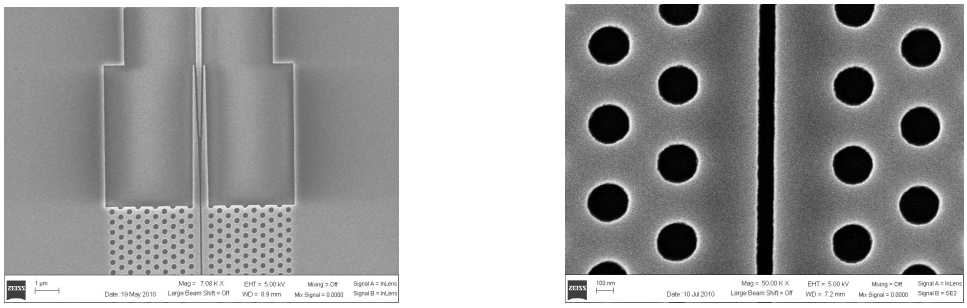

Figure 4: Scanning electron micrograph (SEM) images of photonic crystal slot waveguide devices. (a) shows images of the mode converter taper fabricated for efficient coupling of light from a ridge waveguide into the photonic crystal waveguide. (b) shows magnified image of photonic crystal slot waveguide with dimensions in inset.

For this particular device shown in SEM images in Fig.4, where the lattice constant is *a*=461nm, the design values for air-hole radius and slot width are 0.25*a* and 0.2*a* respectively, i.e. 230nm and 92nm respectively. The fabricated dimensions are 230nm and 96nm respectively, which translates to 0.25*a* and 0.208*a*. Fabricated device dimensions are very close to actual design parameters.

5. EXPERIMENTAL SETUP

A glass cell is mounted on top of the silicon chip. The experimental setup is shown in Fig. 5.

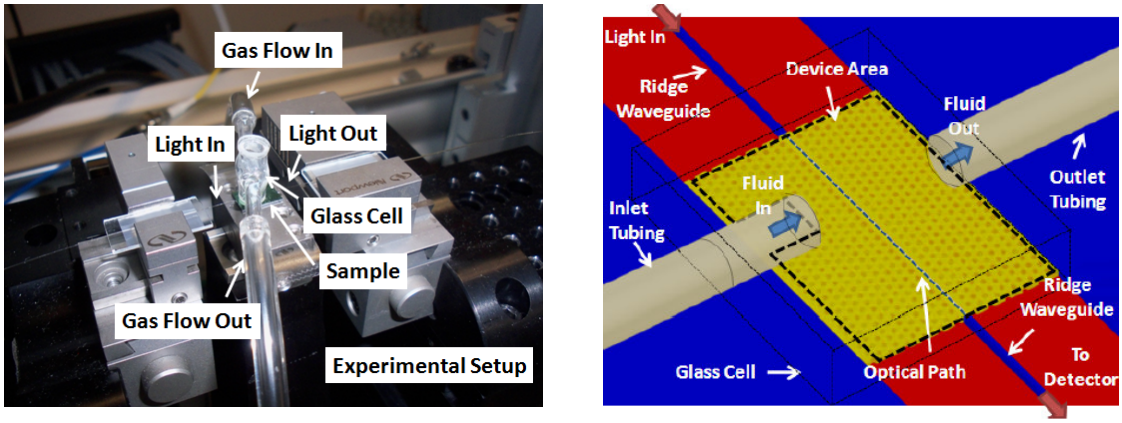

(a) (b)

Figure 5: (a) Experimental setup showing light coupled into sample through optical fiber. Gas flows into and out of the experimental volume through a glass cell as shown. (b) Schematic of the experimental setup showing the alignment of photonic crystal slot waveguide device with respect to the input and output optical fibers and the input and output flow of gas.

The alignment of the glass cell in Fig. 5(a) is compared to the schematic in Fig. 5(b) to show the relative alignment of the gas flow cell with respect to the photonic crystal slot waveguide. Tygon tubes are used to flow gas into and out of the device area. The purpose of the glass cell is simply to have a controlled environment for experiments. For practical field applications, the slot at the middle of the photonic crystal slot waveguide serves as the gas sample cell in our device. Light in coupled into and out of the photonic crystal slot waveguide in the direction perpendicular to the flow of gas through the gas cell. Devices were tested on a Newport six-axis auto-aligning station. Input light from a broadband source (SuperK Versa from NKT Photonics) was TE-polarized and butt-coupled to / from the device with polarization maintaining/ single mode tapered lensed fiber with mode field diameter ~3μm. Transmitted light was analyzed with an optical spectrum analyzer, in presence and absence of methane.

The concentration of methane in nitrogen was varied from 0.1% of permissible exposure limit (PEL) to 4% PEL with a rotameter and absorbance magnitude at 1665.5nm noted as a function of gas concentration. The source gases were nitrogen and 4% methane in nitrogen, both at 20psi. Rotameter settings were made at the calibrated values provided by Matheson Tri-Gas. The absorbance of methane is determined as follows. Let P_a and P_{am} denote the transmission spectrum observed at the output in air and in the presence of methane respectively. Let P_0 denote the input power. If α_a and α_{am} denote absorbance in the absence and presence of methane respectively, thus, for a fixed length d of the photonic crystal slot waveguide, we can write,

$$P_a = P_0 \exp[-\alpha_a d]\ ; \quad P_{am} = P_0 \exp[-\alpha_{am} d];$$

Thus, absorbance of methane = $\Delta\alpha = \alpha_a \sim \alpha_{am} = (1/d) \times \ln(P_a/P_{am})$

6. EXPERIMENTAL RESULTS

The experimental transmission spectrum of the photonic crystal slot waveguide in air is plotted in Fig. 6. The transmission band edge is observed at 1670nm. From the band structure simulation in Fig. 2, the group index is computed and plotted in Fig. 6. The simulated band edge is at ~1668.5nm. In Fig. 7(a), absorbance spectrum variation at 1665.5nm is plotted versus methane concentration.

In Fig. 7(b), absorbance magnitude at 1665.5nm is plotted versus methane concentration. The lowest experimentally determined concentration was 100ppm (parts per million) or 0.2% PEL. As observed in Fig. 7(b), the linear Beer-Lambert law is followed for low concentrations of methane. At higher concentrations, deviations from linearity are observed.

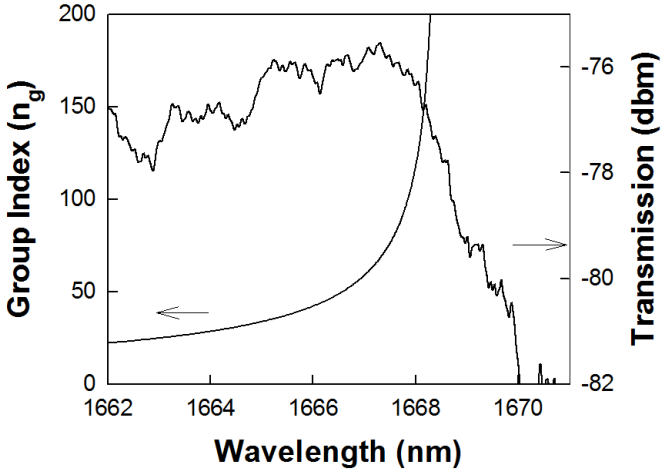

Figure 6: (left axis) Group Index vs. wavelength of the defect guided mode. The device is designed at the operating point where group index n_g=40. (right axis) experimental transmission spectrum of photonic crystal slot waveguide in the presence of methane.

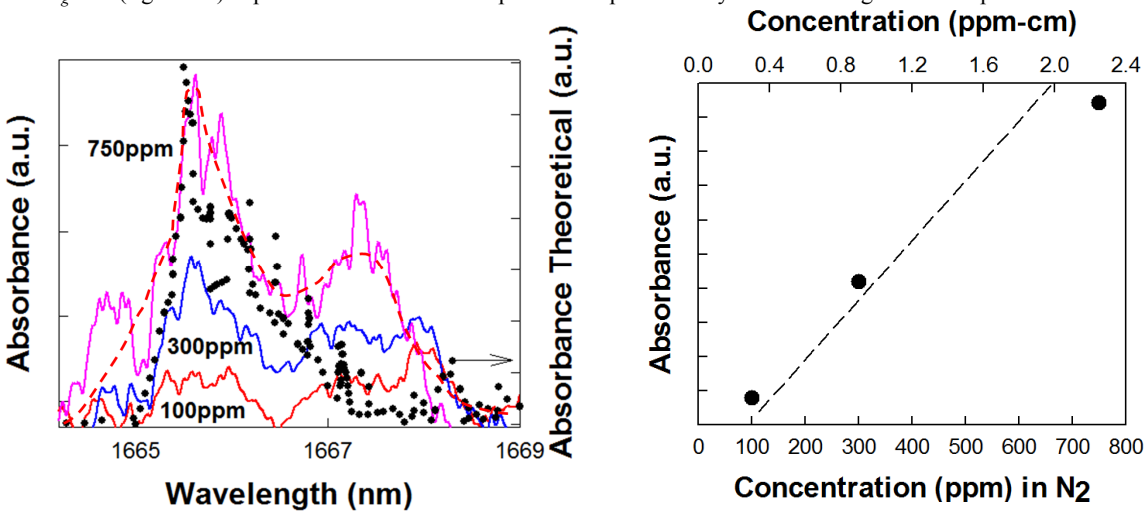

(a) (b)

Figure 7: (a) Experimental absorbance spectrum of methane as a function of concentration in nitrogen by direct absorption spectroscopy. Theoretical absorbance is shown as the black scatter plot. (b) The absorbance magnitude at 1665.5nm is plotted as a function of concentration obtained by direct absorption spectroscopy experimentally.

7. DISCUSSION

As observed in Fig. 7(a), a peak is observed at 1665.5nm with a broad shoulder around 1667.5nm. The theoretical absorbance shown by the scatter plot, has a peak at 1665.5nm. As observed from simulations in Fig. 6, the group index varies rapidly away from the band edge. Near the band edge, the group index is greater than 100, while approximately 5nm away from the band edge, the group index drops to ~25. The higher group index close to the band edge leads to the broad shoulder observed in the experimental absorbance spectrum around 1667.5nm.

The detection limit of the device is thus a strong function of the position of the band edge and hence fabrication imperfections. The smallest number density that can be determined by absorption spectroscopy is given by

$$N_{\min} = \left(\frac{dI}{I_0}\right) / S(\nu) L$$

where,

- dI/I_0 = smallest fractional change in light intensity that can be detected = 5×10^{-4}
- L = effective absorption path length = 300μm x 1000= 30cm
- S(ν) =absorption cross section of methane at 1.665μm = $1.6\times10^{-20}cm^2$ [HITRAN] [7]

$N_{min} = 2.08\times10^{15}$ per cm^3

At NTP, number of molecules per $cm^3 = 6.023\times10^{23} / (22.4\times10^3) = 2.688\times10^{19}$

At 1.665μm, limit of detection for methane for a 300μm long photonic crystal slot waveguide as determined from the above equation is ~40ppm (parts per million) (=0.08% PEL, permissible exposure limit). From Fig. 6, it is observed that the band edge has shifted in experiment by ~1.5nm from design. While the design n_g equals 40, based on band shift due to fabrication imperfections, it is estimated that at 1665.5nm, n_g=30 experimentally. From simulations, the slot enhancement in the photonic crystal slot waveguide is ~12. The effective enhancement achieved in experiment is ~ factor of 360. Based on current experimental results, it is estimated that by greater control on fabrication, the band edge can be shifted closer to the absorbance peak.

Low-loss photonic crystal waveguides up to 1mm have been demonstrated [8]. By increasing the length of the photonic crystal slot waveguide to 1mm, the limit of detection can be reduced by another factor of 3.3 in the near-infrared. Furthermore, dispersive properties of photonic crystals are determined by Maxwell's electromagnetic wave equations that are independent of wavelength. Hence the design demonstrated in the near-infrared on a silicon platform can be readily applied to the mid-infrared wavelength at 3.3μm where methane has higher absorption cross-section $1.3\times10^{-18}cm^2$ [7]. Based on this property, in the mid-infrared, the limit of detection of methane with a 300μm photonic crystal slot waveguide device would be ~400ppb (parts per billion).

In Table 1, the photonic crystal slot waveguide spectroscopy technology for gas spectroscopy is compared with existing optical spectroscopy techniques. It is instructive to note the device demonstrated in this paper is the only demonstrated on-chip near-infrared absorption spectroscopy device for gases.

Table 1: Comparison of photonic crystal slot waveguide spectrometer with other technologies for optical spectroscopy

Property	CRDS [9]	TDLAS [10]	FTIR [11]	PAS [12]	PC Slot Waveguide
On-Chip	No	No	No	No	Yes
Size	~1 cu. ft.	~0.5 cu. ft.	~1.4 cu. ft.	~1 cu. ft.	~0.015 cu. ft
Weight	~28lbs	~6lbs	~24lbs	~33lbs	< 0.1lbs
Power	200 Watt	0.5 Watt	40 Watt	90 Watt	<0.1Watt
Portability	No	No	No	No	Yes
Sensitivity per unit power consumed	40ppm-cm/Watt	50ppm-cm/Watt	200ppm-cm/Watt	450ppm-cm/Watt	0.23ppm-cm/Watt

CRDS: Cavity Ring-Down Spectroscopy; TDLAS: Tunable Diode Laser Absorption Spectroscopy; FTIR: Fourier Transform Infrared Spectroscopy; PAS: Photo-acoustic Spectroscopy; PC: Photonic Crystal

Commercially available optical absorption spectrometers are large, heavy, power consuming and expensive. They can detect only a few species at a time. Systems that detect multiple gases are prohibitively expensive that limits widespread deployment and security. In contrast to devices that consume hundreds of watts of power, our device consumes only few milli-watts, thereby providing orders of magnitude sensitivity efficiencies. Our device offers huge power savings and Cost of Ownership (COO) benefit. The miniaturized platform enables creation of handheld and portable devices, with wide spectral bandwidth, for sensitive and specific remote detection of multiple gases in-situ. Lowest detection limits with power budget and COO benefits presents our photonic crystal slot waveguide absorption spectrometer as a green technology for widespread monitoring of leaks, spills, environmental threats and industrial process conditions.

The silicon compatible platform will ensure high volume and low cost production of devices. The potential commercial application of our versatile miniature spectrometer is any chemical spectroscopy discipline where massively parallel sensing, identification and high throughput analysis are desired, such as quality control of analytical solutions, food and beverages, petroleum, groundwater and trace detection and identification of gases.

8. SUMMARY

In summary, we demonstrated a 300μm long on-chip silicon photonic crystal slot waveguide absorption spectrometer that combines slow light with electric field enhancement for near infrared spectroscopy of methane with sensitivity 100ppm. Remote monitoring is enabled by optical fibers. It is determined that in the mid-infrared, detection limit for methane of 400ppb can be achieved.

ACKNOWLEDGEMENTS

The authors would like to acknowledge the Environmental Protection Agency (EPA) for supporting this work under the Small Business Innovation Research (SBIR) program (EP-D-10-047).

REFERENCES

[1] Mortensen, N.A., Xiao, S.S., "Slow-light enhancement of Beer-Lambert-Bouguer absorption," Applied Physics Letters **90** (14), 141108 (2007).
[2] Chakravarty, S., Topoľančik, J., Bhattacharya, P., Chakrabarti, S., Kang,Y., and Meyerhoff, M.E., "Ion detection with photonic crystal microcavities," Opt. Lett. 30, 2578 (2005).
[3] Notomi, M. "Extremely large group-velocity dispersion of line-defect waveguides in photonic crystal slabs," Physical Review Letters **87**, 253902 (2001).
[4] Xu, Q., Almeida,V.R., Panepucci, R.R., and Lipson,M., "Experimental demonstration of guiding and confining light in nanometer-size low refractive index material," Optics Letters **29**, 1626 (2004).
[5] Chen,X., Jiang,W., Chen, J., Gu, L., Chen,R.T., "20dB enhanced coupling to slot photonic crystal waveguide using multimode interference coupler", Applied Physics Letters 91, 091111 (2007).
[6] Lai, W-C., Chakravarty, S., Wang, X., Lin, C., Chen, R.T., "Photonic Crystal Slot Waveguide Absorption Spectrometer for On-Chip Near-Infrared Spectroscopy of Xylene in Water", Appl. Phys. Lett. (in press)
[7] Rothman, L.S., et al., "The HITRAN 2004 molecular spectroscopic database," Journal of Quantitative spectroscopy and radiative transfer **96**(2), 139 (2005).
[8] O'Faolain, L., Yuan,X., McIntyre,D., Thoms, S., Chong,H., De La Rue, R.M., and Krauss, T.F., "Low-loss propagation in photonic crystal waveguides", Electronics Letters 42 (25), 1454 (2006).
[9] http://www.tigeroptics.com/app/tigeroptics/products/ (Tiger Optics Halo CH4)
[10] http://www.psicorp.com/ (http://www.tdlas.com/index.shtml)
[11] http://www.mksinst.com/product/
[12] http://www.gasera.fi/technology/photoacoustics/solid-phase-pas/